Cable Lobe Detection in a ROV/USV Tethered System Using IMUs and Compliant Buoy-Ballast Equipment

Charly Peraud, Cédric Anthierens, Vincent Hugel

Cable Lobe Detection in a ROV/USV Tethered System Using IMUs and Compliant Buoy-Ballast Equipment

Charly Peraud[1], Cédric Anthierens[1], Vincent Hugel[1]

***Abstract*— This study extends the analysis of a compliant buoy-ballast system integrated into a tethered ROV/USV setup, enhanced with IMU sensors, employing a comprehensive simulation framework for cable dynamics. Building on previous work, this research explores the use of IMU-based measurements to detect risk-prone configurations during ROV operations, specifically focusing on the creation of cable lobes. The study introduces a lobe detection indicator, which compares the signs of horizontal angles obtained from relevant IMUs placed on the cable to identify these configurations. The relevance of this metric was assessed in simulations involving various types of turns during a ROV mission. The results demonstrate that the proposed metric is effective in detecting undesirable lobe formations, and integrating this detection into the winch control system can potentially improve the overall reliability of the ROV/USV system.**

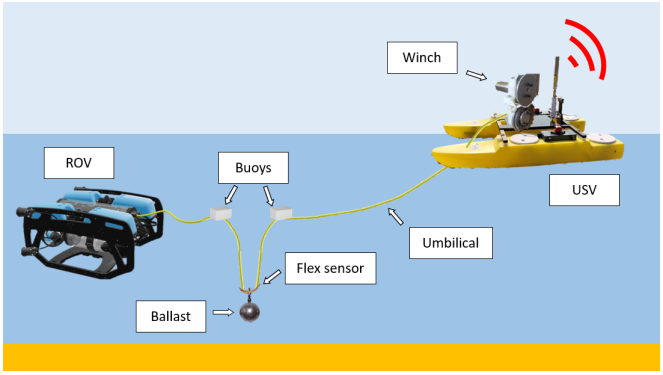

Fig. 1. Compliant buoy-ballast system integrated on the umbilical of a ROV/USV system.

I. Introduction

Robotics is increasingly focusing on deformable bodies for tasks that require compliance, such as handling fragile objects or living cells [1], medical applications [2], bio-inspired locomotion [3], localization in confined environments [4], [5], or trajectory generation for cable-driven robots [6]. In the context of underwater mobile robotics, this paper directly focuses on the umbilical that connects a ROV (Remotely Operated Vehicle) to an USV (Unmanned Surface Vehicle).

A lightweight inspection ROV generally operates at shallow depths (less than 100 meters) and is easy to deploy for various missions [7] such as site exploration, inspection of underwater installations for maintenance purposes, and collection of oceanographic measurements [8], [9], [10], [11]. To expand the ROV's operational range, it can be connected via a cable to an USV that serves as an interface between the ROV in operation and its land-based operator, allowing for remote teleoperation [12], [13].

However, the fact of not being physically on site means that system reliability must be guaranteed, in particular by minimizing cases of communication loss. The presence of this umbilical within the complete system introduces several risks:

- disturbances to the robots (drag forces, jerks, wave propagation, taut cable configuration)
- snagging on natural obstacles or underwater structures
- entanglement with itself

To mitigate these risks, an intuitive solution would involve deploying an appropriate cable length, particularly by incorporating a winch on the USV with onboard intelligence (sensors, algorithms). In this context, previous works of the authors [14], [15] have introduced a system integrated into the umbilical, consisting of two buoys and a ballast, strategically positioned along the cable to naturally form a balanced "V-shape" at rest (Fig.1). By bracing a curvature sensor on the cable over the ballast, the cable length can be controlled by the winch on demand during the mission. This solution has proven effective in reducing disturbances experienced by the ROV due to poor cable management, particularly during straight-line or basic turning trajectories [15]. However, it does not entirely avoid risk-prone configurations, which are especially characterized by the formation of lobes during turns.

In a previous study [16], the development of a comprehensive, realistic, and open-source underwater cable simulator was introduced to replicate the entire system. A new system instrumentation based on Inertial Measurement Unit (IMU) sensors was explored in simulation, and new metrics, such as the turning angle and the inter-buoy distance, were identified as valuable for assessing changes in cable behavior across various scenarios, including straight-line, turning and dive motion for the ROV.

This article aims to exploit these metrics to detect risk-prone situations that may occur during ROV missions. Particular attention is given to turns, which can create lobes in the cable when the robots are in motion.

This paper is organized as follows. Section II presents the physical robotic solution that is replicated in simulation and the simulator that is used for the analysis. Section III provides the simulation setup of the case studies that are replicated in the framework. Section IV details the metrics of interest that will be used for lobe behavior analysis. Section V will discuss the effectiveness of the lobe detection. Finally,

[1]COSMER Laboratory, Univ. de Toulon, France

section VI concludes the study and proposes future work.

II. Robotic Solution and Simulator

A. Robotic Solution

The considered ROV is the heavy configuration of the BlueROV2 equipped with eight T200 thrusters. A 50-meter umbilical cable ensures communication between the ROV and the surface mobile station, which is a 120 cm long Hydrone-based USV equipped with two T200 thrusters (Fig.2). Human-machine communication is established via Wi-Fi with the USV, which transmits and collects the necessary information to and from the ROV. The umbilical is a 4 mm diameter twisted pair cable with neutral buoyancy. The compliant part of the V-shape system is positioned along the cable, 40 cm from the ROV, and consists of two buoys spaced 120 cm apart and a 75g weight placed between. At rest, this section naturally forms a V shape with approximately 20 cm between the buoys. This shape can easily open up when the cable is under tension. To detect this opening, which indicates tension caused by drag, current, or the ROV moving away from the USV, a curvature sensor is placed at the ballast. Typically, as the ROV moves further away, the increasing distance between the buoys signals the winch to release more cable accordingly.

Fig. 2. ROV (Bluerov2) and USV (Hydrone-based) of the system.

B. Cable instrumentation

To further leverage this custom instrumentation, IMUs can be placed on the V-shaped part to replace the curvature sensor, which only provides scalar information. Thus, vectorial data can be obtained, which reveals out-of-plane configurations of the V during motion, giving insight into the geometry of the cable's departure point on the ROV side. The orientation of the cable strands within the V-shape system can also be determined, which helps to reconstruct the inter-buoy distance, indicating tension in the cable.

The implementation of IMUs on the actual system can be achieved using BMX160 sensors mounted on evaluation boards and attached to the cable with brackets produced via additive manufacturing. These I2C IMUs collect data from 3 accelerometers, 3 gyroscopes, and 3 magnetometers at a frequency of up to 100 Hz.

To obtain information on the cable's departure angle from the winch, an instrumented flexible sheath with an integrated IMU will be used, aligned with the cable's direction.

C. Simulation Framework

To model the overall system in an underwater environment, a comprehensive cable dynamics simulation framework developed in [16] is used in this work. This framework considers variable-length cables and allows incorporating elements such as buoys, ballast or IMU sensors. To address length variations induced by the winch during the cable management, the methodology proposed in [17] is adopted and a Newton-Raphson iteration algorithm is used for solving. Both ROV and USV motions are incorporated using hydrodynamics models from [18]. External disturbances can also be accounted for, such as marine current maps, to represent real-world operating conditions.

III. Case Studies

The system was replicated in the simulator (Fig. 3). To represent the flexibility at the winch output proposed by the technological solution used, the winch was placed at a point distinct from that of the USV in the simulation. A finer mesh was applied near the buoys, ballast, winch, and robots to enhance simulation accuracy, especially in cable sections prone to sharp bending.

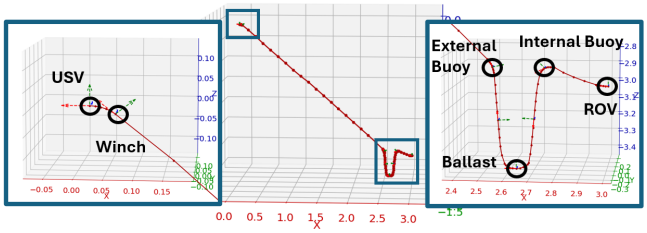

Fig. 3. Complete system replication in the simulation framework

The behavior of the winch, which is similar to that of a DC motor (a second-order low-pass system where the electrical time constant is negligible compared to the mechanical time constant), will be modeled as a first-order low-pass system with a static gain of $K = 1$ and a time constant of $\tau = 0.16\ s$.

In the following simulations, the USV will be considered stationary, imposing boundary conditions of zero velocity throughout the simulation. The numerical values for the ROV-specific coefficients (damping, inertia, added mass) are based on the literature [19]. The degrees of freedom for the ROV are managed by PID controllers, which have been pre-tuned. The system will therefore be controlled with 7 degrees of freedom: 6 for the ROV (3 translations and 3 rotations), and 1 for the winch (reeling speed).

Two scenarios will be studied in this work: a Simple Turn and a Zigzag Turn, the latter involving alternating turns in opposite directions to create a zigzag pattern. Both scenarios start with the ROV positioned 3 meters in front of the USV, at a depth of 3 meters, with 5.35 meters of cable deployed, and the V-shape system having reached its resting configuration, as shown in Fig. 3. The winch is actuated according to the buoy-gap control mode described in [14], employing

a proportional-derivative controller. The different stages of commands for the ROV are presented in Tab. I :

TABLE I
ROV STAGES [TIME, SURGE, YAW], UNITS:[s, m/s, rad/s]

Trajectory	Simple Turn	Zigzag Turn
Stage	[t, s, y]	[t, s, y]
0	[0, 0, 0]	[0, 0, 0]
1	[2, 0.2, 0]	[2, 0.2, 0]
2	[3, 0.2, 0]	[3, 0.2, 0]
3	[4, 0.2, 0.2]	[4, 0.2, 0.2]
4	[9, 0.2, 0.2]	[9, 0.2, 0.2]
5	[10, 0.2, 0]	[10, 0.2, 0]
6	[20, 0.2, 0]	[20, 0.2, 0]
7	[21, 0, 0]	[21, 0.2, −0.2]
8	[31, 0, 0]	[31, 0.2, −0.2]
9	-	[32, 0.2, 0]
10	-	[85, 0.2, 0]

IV. METRICS OF INTEREST

Figure 4 presents several configurations that may occur during a turning motion. In Configuration 1, distributing the cable ensures the proper functioning of the V-shape system. In Configuration 2, a lobe begins to form, and adding more cable appears to enlarge this lobe. In Configuration 3, although the lobe persists, the situation reverts to conditions similar to Configuration 1. Thus, it seems that the current winch operation is not optimized for Configuration 2. Detecting such scenarios would be advantageous for adjusting the control strategy accordingly.

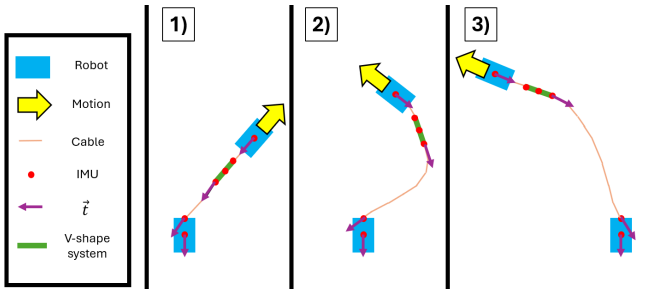

Fig. 4. Decomposition of a turning motion during an ROV/USV mission equipped with the V-shape system

In [16], the horizontal relative angle between an IMU i and a reference IMU was introduced, denoted as $\boldsymbol{\alpha_i}$, which is defined from the scalar product of the horizontal projections of vectors $\boldsymbol{t_i}$ and $\boldsymbol{t_{ref}}$. The USV is chosen as the reference to focus on the previously mentioned angles, specifically the horizontal angles of the external buoy and the winch (Fig. 3), denoted as $\boldsymbol{\alpha_{eb}}$ and $\boldsymbol{\alpha_w}$, respectively. The horizontal angle of the ROV $\boldsymbol{\alpha_r}$ will also be analyzed, as it reflects the dynamics of the cable.

Upon examining these data, it was observed that Configurations 1 and 3 show angles $\boldsymbol{\alpha_{eb}}$ and $\boldsymbol{\alpha_w}$ with the same sign, while Configuration 2 exhibits different signs. A lobe detection indicator will be developed, based on the comparison of the signs of $\boldsymbol{\alpha_{eb}}$ and $\boldsymbol{\alpha_w}$, and the resulting signal will be discussed.

The angular difference between the external buoy and the winch, denoted as $\boldsymbol{\alpha_{eb,w}}$, is high as it indicates the amplitude of the lobe in the longest segment of the cable, between the V and the winch. Additionally, the angular difference between the ROV and the external buoy, denoted as $\boldsymbol{\alpha_{r,eb}}$ provides insight into the direction of bending of the V-shape system.

V. RESULTS AND DISCUSSION

Figures 5 and 6 present the results of the Simple Turn and Zigzag Turn simulations. At the top of each figure, the IMU-based estimated and simulated inter-buoy distances are shown, illustrating the overall behavior of the V-shape system. In the middle section, the lobe detection signal and the horizontal angles of the ROV, the external buoy and the winch are depicted. At the bottom, the differences between the horizontal angles are presented.

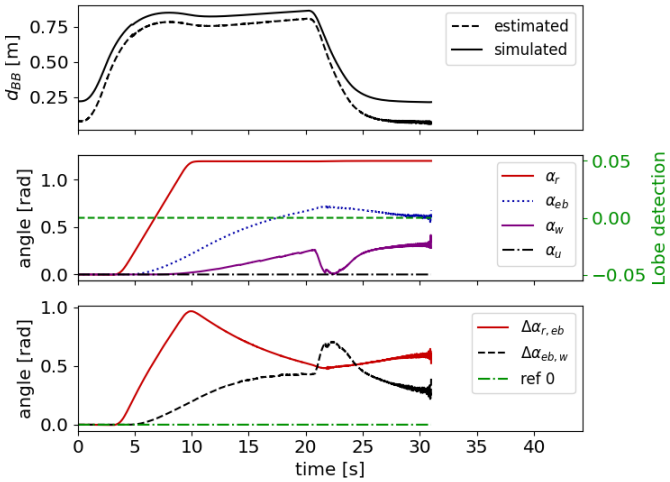

Fig. 5. Inter-buoy distance (IMU-based and simulated), horizontal angles of the ROV, external buoy and winch (IMU-based) with the lobe detection signal, and difference between horizontal angles (IMU-based) during Simple Turn simulation, published online in August 2024, https://youtu.be/garHpUqI6H4

During the Simple Turn simulation (Fig. 5), the inter-buoy distance accurately reflects the behavior of the V-shape, increasing during the turn and decreasing when the movement stops, gradually returning to its resting configuration. The difference in horizontal angles $\boldsymbol{\alpha_{r,eb}}$ seems to reflect the V-shape's behavior to follow the natural curvature imposed by the robot's turning movement. However, it retains a natural curvature due to its inherent compliance, which forces the system to return to a plane. The difference in horizontal angles $\boldsymbol{\alpha_{eb,w}}$ also increases as the turn progresses, reflecting the emergence of a curvature in the longest segment of the cable. However, the lobe detection signal does not indicate a risk-prone configuration because the cable remains in a favorable setup for the winch controller (Configuration 1 of Fig. 4).

This analysis remains consistent with the data from the Zigzag Turn simulation (Fig. 6) during the initial phase of the movement (up to 20 seconds). However, as the ROV changes direction, indicated by the variable $\boldsymbol{\alpha_r}$, it gradually

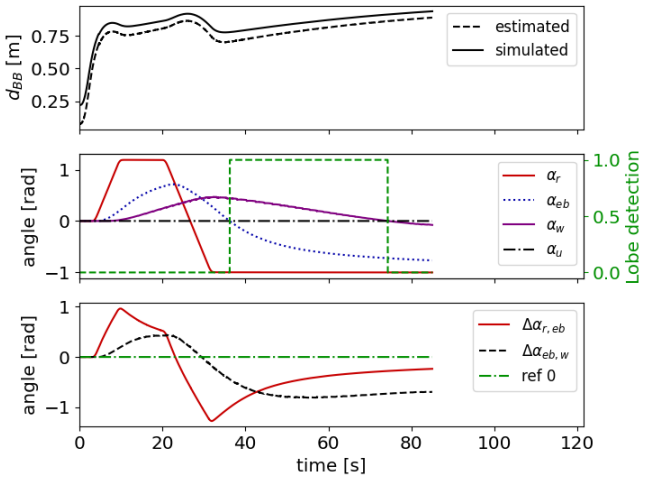

Fig. 6. Inter-buoy distance (IMU-based and simulated), horizontal angles of the ROV, external buoy and winch (IMU-based) with the lobe detection signal, and difference between horizontal angles (IMU-based) during Zigzag Turn simulation, published online in August 2024, https://youtu.be/RAcVYmOF8qk

affects the orientation of the external buoy $\boldsymbol{\alpha_{eb}}$. This leads the system into Configuration 2, shown in Fig. 4, where an undesirable lobe begins to form in the cable, as evidenced by the increase of the amplitude of $\boldsymbol{\alpha_{eb,w}}$. This configuration is detected by the lobe detection signal (starting at 36 seconds). As the ROV continues its turn, the system shifts to Configuration 3 (at 74 seconds), a scenario more favorable for the current winch control setup.

Thus, the lobe detection signal appears effective at identifying risk-prone configurations, and incorporating it into a more advanced winch controller could potentially reduce their occurrence. Additionally, interpreting $\boldsymbol{\alpha_{eb,w}}$ helps assess the amplitude of the lobe, highlighting the necessity of reducing it.

VI. Conclusion

This study aims to build on previous research that analyzed a compliant buoy-ballast solution equipped with IMUs and integrated along the cable of a ROV/USV tethered system within a comprehensive simulation framework for cable dynamics. New simulations involving simple turns and zigzag maneuvers were conducted using this framework. Metrics introduced in the previous study, specifically the distance between the buoys and the horizontal angles, are employed to better characterize the cable's behavior.

The analysis of the system's natural movement during a turn reveals configurations prone to lobe formation, which poses a significant risk to system reliability. This study proposes the monitoring of the horizontal angles between the external buoy and the USV, and between the winch and the USV, as obtained from the IMUs, to detect such configurations. Simulation results show that the sign comparison of these angles provides a relevant lobe detection signal. This signal can then be used to inform the winch controller, enabling it to adjust commands accordingly. Additionally, the difference between these angles helps assess the amplitude of the lobe, highlighting the importance of the loop being currently formed.

Future work will focus on refining the winch control algorithm to mitigate lobe formation when detected. New control strategies that integrate both the USV and the winch may be proposed to enhance system reliability during exploration missions. Additionally, the development of a mathematical model that incorporates the horizontal measured angles on both sides of the V-shape segment of the cable, and current cable length could provide valuable insights into the determination of the relative position between the ROV and the USV, which is a significant challenge in underwater robotics.

References

[1] Josh Pinskier, Xing Wang, Lois Liow, Yue Xie, Prabhat Kumar, Matthijs Langelaar, and David Howard. Diversity-Based Topology Optimization of Soft Robotic Grippers. *Advanced Intelligent Systems*, 6(4):2300505, April 2024.

[2] Mostafa Sayahkarajy and Hartmut Witte. Soft Medical Robots and Probes: Concise Survey of Current Advances. *DESIGN, CONSTRUCTION, MAINTENANCE*, 3:263–278, December 2023.

[3] Chee-Meng Chew, Qing-Yuan Lim, and K. S. Yeo. Development of propulsion mechanism for Robot Manta Ray. In *2015 IEEE International Conference on Robotics and Biomimetics (ROBIO)*, pages 1918–1923, Zhuhai, December 2015. IEEE.

[4] A. Borgese, D. C. Guastella, G. Sutera, and G. Muscato. Tether-Based Localization for Cooperative Ground and Aerial Vehicles. *IEEE Robotics and Automation Letters*, 7(3):8162–8169, July 2022. Conference Name: IEEE Robotics and Automation Letters.

[5] J. Drupt, C. Dune, A. I. Comport, S. Sellier, and V. Hugel. Inertial-Measurement-Based Catenary Shape Estimation of Underwater Cables for Tethered Robots. In *2022 IEEE/RSJ International Conference on Intelligent Robots and Systems (IROS)*, October 2022.

[6] Peng Liu, Hongwei Ma, Xiangang Cao, Xuhui Zhang, Xuechao Duan, and Zhen Nie. Minimum Dynamic Cable Tension Workspace Generation Techniques and Cable Tension Sensitivity Analysis Methods for Cable-Suspended Gangue-Sorting Robots. *Machines*, 11(3):338, March 2023.

[7] R. Capocci, G. Dooly, E. Omerdić, J. Coleman, T. Newe, and D. Toal. Inspection-Class Remotely Operated Vehicles—A Review. *Journal of Marine Science and Engineering*, 5(1):13, March 2017.

[8] Ingunn Nilssen, Øyvind Ødegård, Asgeir J. Sørensen, Geir Johnsen, Mark A. Moline, and Jørgen Berge. Integrated environmental mapping and monitoring, a methodological approach to optimise knowledge gathering and sampling strategy. *Marine Pollution Bulletin*, 96(1-2):374–383, July 2015.

[9] Chenyu Zhao, Philipp Thies, and Lars Johanning. Offshore inspection mission modelling for an ASV/ROV system. *Ocean Engineering*, 259:111899, July 2022.

[10] Darryn Sward, Jacquomo Monk, and Neville Barrett. A Systematic Review of Remotely Operated Vehicle Surveys for Visually Assessing Fish Assemblages. *Frontiers in Marine Science*, 6:134, April 2019.

[11] Nadir Kapetanović, Antonio Vasilijević, ula Na, Krunoslav Zubčić, and Nikola Mišković. Marine Robots Mapping the Present and the Past: Unraveling the Secrets of the Deep. *Remote Sensing*, 12(23):3902, January 2020. Number: 23 Publisher: Multidisciplinary Digital Publishing Institute.

[12] Chenyu Zhao, Philipp Thies, Lars Johanning, and J. Cowles. Modelling and assessment of ROV capacity within an autonomous offshore intervention system. pages 755–759. September 2020.

[13] Nadir Kapetanović, Kristijan Krčmar, Nikola Miskovic, and ula Na. Tether Management System for Autonomous Inspection Missions in Mariculture Using an ASV and an ROV. *IFAC-PapersOnLine*, 55:327–332, November 2022.

[14] Ornella Tortorici, Cédric Anthierens, and Vincent Hugel. A New Flex-Sensor-Based Umbilical-Length Management System for Underwater Robots. In *2023 European Conference on Mobile Robots (ECMR)*, pages 1–6, Coimbra, Portugal, September 2023. IEEE.

[15] Ornella Tortorici, Charly Péraud, Cédric Anthierens, and Vincent Hugel. Automated Deployment of an Underwater Tether Equipped with a Compliant Buoy–Ballast System for Remotely Operated Vehicle Intervention. *Journal of Marine Science and Engineering*, 12(2):279, February 2024.

[16] Charly Peraud, Martin Filliung, Cedric Anthierens, Claire Dune, Nicolas Boizot, and Vincent Hugel. IMU-based Monitoring of Buoy-Ballast System through Cable Dynamics Simulation. *2024 IEEE/RSJ International Conference on Intelligent Robots and Systems (IROS)*, 2024.

[17] J.L. Tang, G.X. Ren, W.D. Zhu, and H. Ren. Dynamics of variable-length tethers with application to tethered satellite deployment. *Communications in Nonlinear Science and Numerical Simulation*, 16(8):3411–3424, August 2011.

[18] T.I. Fossen. *Handbook of Marine Craft Hydrodynamics and Motion Control*. Wiley, 2021.

[19] Chu-Jou Wu and B Eng. 6-DoF Modelling and Control of a Remotely Operated Vehicle. Master's thesis, College of Science and Engineering, Flinders University, 2018.